Environmental Science & Technology

Article

Cite This: Environ. Sci. Technol. 2019, 53, 1822−1833

pubs.acs.org/est

Assessing Contributions of Agricultural and Nonagricultural Emissions to Atmospheric Ammonia in a Chinese Megacity

Yunhua Chang,[†,#] Zhong Zou,[‡,#] Yanlin Zhang,[*,†] Congrui Deng,[*,‡] Jianlin Hu,[§] Zhihao Shi,[§] Anthony J. Dore,[∥] and Jeffrey L. Collett, Jr.[⊥]

[†]Yale-NUIST Center on Atmospheric Environment, Nanjing University of Information Science & Technology, Nanjing 210044, P. R. China

[‡]Department of Environmental Science & Engineering, Institute of Atmospheric Sciences, Fudan University, Shanghai 200433, P. R. China

[§]School of Environmental Science and Engineering, Nanjing University of Information Science & Technology, Nanjing 210044, P. R. China

[∥]Centre for Ecology & Hydrology Edinburgh, Bush Estate, Penicuik, Midlothian EH26 0QB, United Kingdom

[⊥]Department of Atmospheric Science, Colorado State University, Fort Collins, Colorado 80523, United States

Supporting Information

ABSTRACT: Ammonia (NH_3) is the predominant alkaline gas in the atmosphere contributing to formation of fine particles—a leading environmental cause of increased morbidity and mortality worldwide. Prior findings suggest that NH_3 in the urban atmosphere derives from a complex mixture of agricultural (mainly livestock production and fertilizer application) and nonagricultural (e.g., urban waste, fossil fuel-related emissions) sources; however, a citywide holistic assessment is hitherto lacking. Here we show that NH_3 from nonagricultural sources rivals agricultural NH_3 source contributions in the Shanghai urban atmosphere. We base our conclusion on four independent approaches: (i) a full-year operation of a passive NH_3 monitoring network at 14 locations covering urban, suburban, and rural landscapes; (ii) model-measurement comparison of hourly NH_3 concentrations at a pair of urban and rural supersites; (iii) source-specific NH_3 measurements from emission sources; and (iv) localized isotopic signatures of NH_3 sources integrated in a Bayesian isotope mixing model to make isotope-based source apportionment estimates of ambient NH_3. Results indicate that nonagricultural sources and agricultural sources are both important contributors to NH_3 in the urban atmosphere. These findings highlight opportunities to limit NH_3 emissions from nonagricultural sources to help curb $PM_{2.5}$ pollution in urban China.

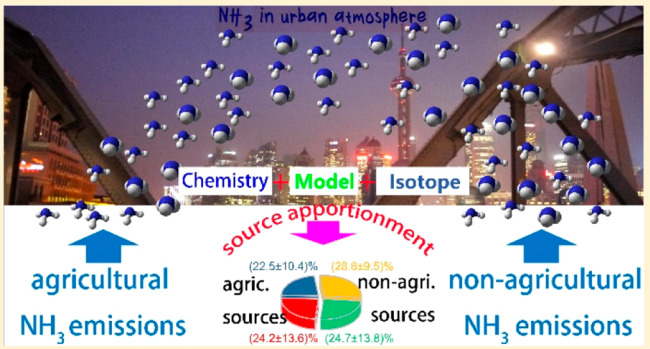

1. INTRODUCTION

Atmospheric ammonia (NH_3) is the predominant alkaline gas in the atmosphere and actively involved in atmospheric chemistry. In reactions with sulfuric acid and nitric acid, formed via the oxidation of SO_2 and NO_x, respectively, NH_3 contributes to the formation of NH_4^+ salts, which typically make up from 20% to 80% of atmospheric particulate matter with an aerodynamic diameter less than 2.5 μm ($PM_{2.5}$).[1−5] This fine particle formation has led to huge health and economic costs.[6−10]

There is an increasing importance of NH_3 emissions relative to SO_2 and NO_x worldwide due to relatively slow reduction of NH_3 emissons.[11−17] Over 90% of NH_3 emissions in China, the United States, and many European countries result from agriculture, mainly including livestock production and NH_3-based fertilizer application;[6,13,15,18−22] thus, agricultural NH_3 emissions are often blamed for high levels of ammonium-containing $PM_{2.5}$.[1,6,7,23,24] However, in urban areas where agricultural activities are mostly absent, a growing body of evidence suggests that nonagricultural activities like wastewater treatment,[25] coal combustion,[26] solid garbage,[27] vehicular exhaust,[28] and urban green space[29] also contribute to NH_3 emissions.[30] For example, large vehicular NH_3 emissions from noble metal-based three-way catalysts (TWCs) have been detected in chassis dynamometer vehicle experiments, road tunnel tests, and ambient air measurements dating back to the 1980s.[31−42] Nevertheless, Yao et al.[43] and Teng et al.[29] suggest that vehicular NH_3 emissions can be neglected and proposed urban green spaces as the dominant contributor to urban

Received: October 23, 2018
Revised: January 5, 2019
Accepted: January 15, 2019
Published: January 15, 2019

DOI: 10.1021/acs.est.8b05984
Environ. Sci. Technol. 2019, 53, 1822−1833

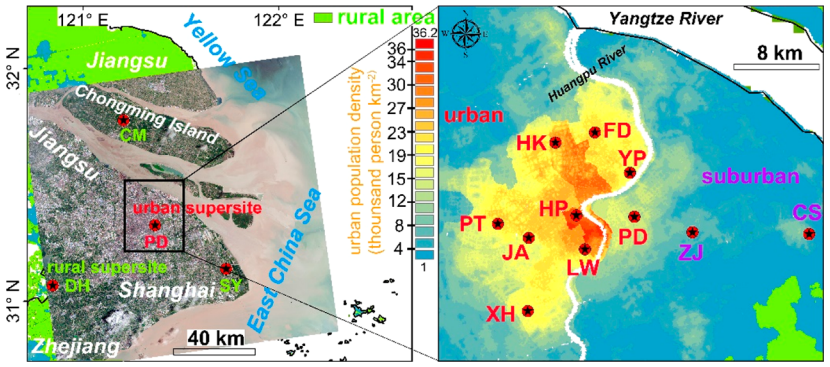

Figure 1. Shanghai passive ammonia monitoring network. The natural-color satellite image in the left panel shows the urban area of Shanghai in 2016, along with its major island Chongming. The right panel presents the population density in Shanghai, which was retrieved from a newly released high-resolution (100 × 100 m^2 per pixel) population map of China in 2010 (worldpop.org.uk).

atmospheric NH_3 in North America and Northern China. There remains a long-standing and ongoing controversy regarding the relative contribution of agricultural and nonagricultural NH_3 emissions in the urban atmosphere.[44−46]

In China, while there have been no long-term and nationwide NH_3 monitoring studies like the U.S. passive Ammonia Monitoring Network (AMoN, http://nadp.sws.uiuc.edu/amon) affiliated with the National Atmospheric Deposition Program (NADP),[47−49] numerous researchers have measured NH_4^+ concentrations in wet deposition (i.e., precipitation) for more than 30 years.[50,51] The data show that the annual flux of NH_4^+ in wet deposition in China has increased in conjunction with the growth in animal production and fertilizer application.[17,50,52,53] Further, China's recent economic boom has been coupled with accelerated urbanization.[54,55] In 1978 less than 20% of Chinese residents lived in cities. The population of its cities has quintupled over the past 40 years, reaching 813 million or nearly 60% of the total population.[56] At present, there are three super-regions or city clusters in China: the Pearl River Delta (PRD), next to Hong Kong; the Yangtze River Delta (YRD), which surrounds Shanghai; and Jing-jin-ji (J^3), centered on Beijing.[57] In particular, the YRD region is arguably the most concentrated set of adjacent urban conurbations in the world.[58] Huge cities place huge demands on resource consumption and associated nonagricultural NH_3 emissions.[44] For example, the region has continuously experienced double-digit growth in auto sales since 2009.[36] The expanding motor vehicle population in its cities, in turn, is reshaping the urban atmospheric composition.[59,60] Meanwhile, the vast rural areas of the YRD region are dominated by fluvial plains with fertile soil, and abundant production of rice and tea.[22] According to Huang et al.,[22] livestock production, N-fertilizer application, and nonagricultural sources (including sewage treatment, waste landfills, and human discharge) in the YRD region in 2007 comprise 48%, 40%, and 12% of the total 459 kt NH_3 emissions, respectively. The interplay of agricultural and nonagricultural NH_3 emissions in the region provides an ideal study area to investigate their impact on ambient NH_3 concentrations over time.

Taking Shanghai as an example, the present study aims to systematically elucidate the role of nonagricultural NH_3 emissions contributing to ambient NH_3 in the urban atmosphere through (1) investigating the spatial and temporal variability of NH_3 concentrations across various land use categories, (2) interpreting the consistency or discrepancy of NH_3 concentrations between field measurements and chemical transport model simulations, and (3) using stable isotopes as a tool to quantify source category contributions to ambient NH_3 concentrations in the rural and urban atmospheres.

2. MATERIALS AND METHODS

2.1. Site Description. The Yangtze River Delta or YRD region encompasses the nation's largest population center, Shanghai, and major agricultural fields in eastern China. In order to obtain information regarding the spatial and temporal variability of NH_3 concentrations in Shanghai, we established a regional monitoring network of 14 sites covering urban (FD, HK, YP, HP, PT, JA, LW, XH, and PD), suburban (ZJ and CJ), and rural (DH, SY, and CM) landscapes (Figure 1). Of particular importance are PD and DH, which also serve as supersites intended to represent urban and rural settings, respectively. In Shanghai, all ten state-control stations (SCS) of China's Ministry of Environmental Protection were utilized. The advantages of selecting these SCS sites include (i) their deliberate locations away from point and local sources of pollution, such as transportation corridors, agricultural fields, livestock operations, and industrial emissions; (ii) they have well-trained staff with long-term employment to sustain continuous measurements; and (iii) they are equipped with refrigerators so that the collected samples can be quickly stored to prevent potential contamination or sample degradation. More detailed site descriptions can be found elsewhere.[36,61] The meteorology in Shanghai is typical of a subtropical monsoon system with four distinct seasons. A summary of the average meteorological conditions can be found in Supporting Information, SI, Figure S1.

2.2. Field Sampling. In order to obtain the spatial distributions of NH_3 concentrations over the Shanghai region, from May 2014 to June 2015, weekly Ogawa PSDs (passive sampling devices, Ogawa, FL, U.S.A.) were deployed at each site (from March 2017 to March 2018 for CM and SY sites) under the protection of an opaque shelter for collecting ambient NH_3. Between June and August of 2014, two Ogawa PSDs were deployed for monthly collection at the urban PD site and the rural DH site for N isotopic analysis of NH_3. The Ogawa PSD consists of a solid cylindrical polymeric body (2 cm diameter, 3 cm long) housing a citric acid-coated glass fiber disk at each end as a duplicate to trap NH_3.[48] All PSD components (including filters) were purchased from Ogawa U.S.A., and sampling procedures provided by the manufacturer (http://www.ogawausa.com) were strictly followed through-

DOI: 10.1021/acs.est.8b05984
Environ. Sci. Technol. 2019, 53, 1822−1833

Table 1. Mass Concentrations and Isotopic Signatures ($\delta^{15}N$) of Major NH_3 Sources

category	subcategory	NH_3 ($\mu g\ m^{-3}$)	$\delta^{15}N$-NH_3 (‰)	N	reference
livestock breeding (LB)	pig breeding	462.2 to 1502.8	−31.7 to −27.1	7	65
N-fertilizer application (FA)	urea	165.6 to 623.7	−52.0 to −47.6	5	65
urban waste (UW)	solid waste	271.2 to 542.4	−37.6 to −29.9	8	65
	wastewater	127.2 to 258.5	−41.9 to −39.2	8	65
	human excreta	3238.0 to 6211.0	−39.6 to −37.3	8	61
fossil fuel-related (FF)	vehicle (road tunnel)	33.2 to 87.4	−17.8 to −9.6	8	65
	power plant (NH_3 slip)	not available	−14.6, −11.3	2	76

out the campaign. After exposure, the filters were transferred with tweezers into plastic vials (15 mL) and stored at −18 °C immediately. The samples were delivered to the analytical laboratory monthly. The average relative percent difference between duplicate Ogawa PSD samples was 5.5%.

In order to relate temporal variations of NH_3 concentrations to potential NH_3 sources, the PD (urban), and DH (rural) sites were equipped with a Monitor for AeRosols and Gases (MARGA, Applikon B.V., NL), allowing continuous characterization of the inorganic components of $PM_{2.5}$ (NH_4^+, NO_3^-, SO_4^{2-}, Cl^-, Na^+, K^+, Ca^{2+}, Mg^{2+}) and water-soluble gases (NH_3, SO_2, HCl, HONO, and HNO_3) at hourly resolution.[62] This effort builds upon our earlier effort[36] to look at the influence of on-road traffic on ambient NH_3 variability with different meteorology at the PD site. Details of the MARGA instrument and its performance can be found elsewhere.[36] To complement the information obtained from the MARGA monitoring campaign, additional measurements of tailpipe-emitted NH_3 from 19 different vehicles equipped with three-way catalytic converters were carried out in Nanjing, a megacity in the western Yangtze River Delta region, during April 2016, following a method described elsewhere[63] and briefly summarized in SI Text S1.

2.3. Laboratory Analysis. NH_4^+ concentrations in the H_2SO_4 absorbing solutions were measured using a Dionex ICS-5000$^+$ system (Thermo Fisher Scientific, Sunnyvale, U.S.A.) at the clean laboratory (class 1000) of Yale-NUIST Center on Atmospheric Environment. The IC system was equipped with an automated sampler (AS-DV). NH_4^+ in solutions was measured using an IonPac CG12A guard column and CS12A separation column with an aqueous methanesulfonic acid (MSA, 30 mM L^{-1}) eluent at a flow rate of 1 mL min^{-1}. For the Ogawa passive samples, each filter pad was soaked in 8 mL deionized water (18 MΩ·cm) in a 15 mL vial for 30 min with occasional shaking. Concentrations of NH_4^+ in extracts were analyzed using an ion chromatography system (883 Basic IC plus, Metrohm Co., Switzerland) equipped with a Metrosep C4/4.0 cation column. The eluent was 1.0 mmol L^{-1} HNO_3 + 1.0 mmol L^{-1} 2,6-pyridine dicarboxylic acid. The detection limit for NH_4^+ was 2.8 $\mu g\ L^{-1}$, corresponding to an ambient NH_3 concentration of 0.1 ppb for a seven-day sample.

For isotopic analysis, a robust and quantitative chemical method was used to determine $\delta^{15}N$-NH_4^+ based on the isotopic analysis of nitrous oxide (N_2O),[64] as detailed and successfully applied in our previous studies.[61,65] One of the advantages of this method is that it is more suitable for low volume samples including those with low nitrogen concentration. The standard deviation of $\delta^{15}N$ measurements determined from the replicates is less than 0.3‰.

2.4. Ammonia Modeling. The Community Multiscale Air Quality (CMAQ, v5.0.1) chemical transport model was used to simulate hourly NH_3 and NH_4^+ concentrations in Shanghai with a 12 × 12 km^2 grid resolution.[66] Meteorological inputs were generated with the Weather Research and Forecasting (WRF v3.6.1) model and the National Centers for Environmental Prediction FNL Operational Model Global Tropospheric Analyses. The tropospheric analyses data set was used to provide initial and boundary conditions. A multiresolution emission inventory for China developed by Tsinghua University (http://www.meicmodel.org) was used to define monthly anthropogenic emissions from China. Anthropogenic emissions in 2012 including NH_3, SO_2, NO_x, volatile organic compounds, and PM were regridded to the model grids. Open biomass burning emissions were generated from the Fire INventory from NCAR, which is based on satellite observations.[66] Dust and sea salt emissions were generated online during the CMAQ simulations. Biogenic emissions were generated using the Model for Emissions of Gases and Aerosols from Nature (v2.1).[66] The model configurations of CMAQ and WRF are similar to those utilized in a previous nationwide study.[66]

2.5. Bayesian Mixing Model. Isotopic mixing models allow us to estimate the proportional contributions of multiple sources (emission sources of NH_3 in this study) within a mixture (the ambient NH_3 in this study).[67] By explicitly reflecting the uncertainties associated with multiple sources, isotope fractionation, and isotopic signatures, the application of Bayesian methods to stable isotope mixing models is able to generate robust probability estimates of source proportions, being more appropriate in natural systems than simple linear mixing models.[68,69] Here a novel Bayesian methodology for analyzing mixing models implemented in the software package SIAR (Stable Isotope Analysis in R)[70] was used to resolve multiple NH_3 source categories by generating potential solutions of source apportionment as true probability distributions. The generation of such source contribution probability distributions is helpful in estimating likely ranges of source contributions when the system solution is under-constrained (i.e., the number of sources exceeds the number of different isotope system tracers +1). The SIAR package is available to download from the packages section of the Comprehensive R Archive Network site (CRAN)−http://cran.r-project.org/, and has been widely applied in a number of fields.[71−75] Model frame and computing methods are detailed in SI Text S2.

A comprehensive pool of isotopic source signatures of NH_3 (IS_NH_3) has been established in our previous work[65] with the exception of "NH_3 slip from coal-fired power plant".[76] These IS_NH_3 are typically found to lie between −50‰ and −10‰, with occasional overlap between signatures from different source types.[65,77] The NH_3 emissions were defined by four distinct source categories (Table 1): livestock breeding (−29.1 ± 1.7‰), N-fertilizer application (−50.0 ± 1.8‰; urea application), combustion-related sources (−14.0 ± 2.7‰;

DOI: 10.1021/acs.est.8b05984
Environ. Sci. Technol. 2019, 53, 1822−1833

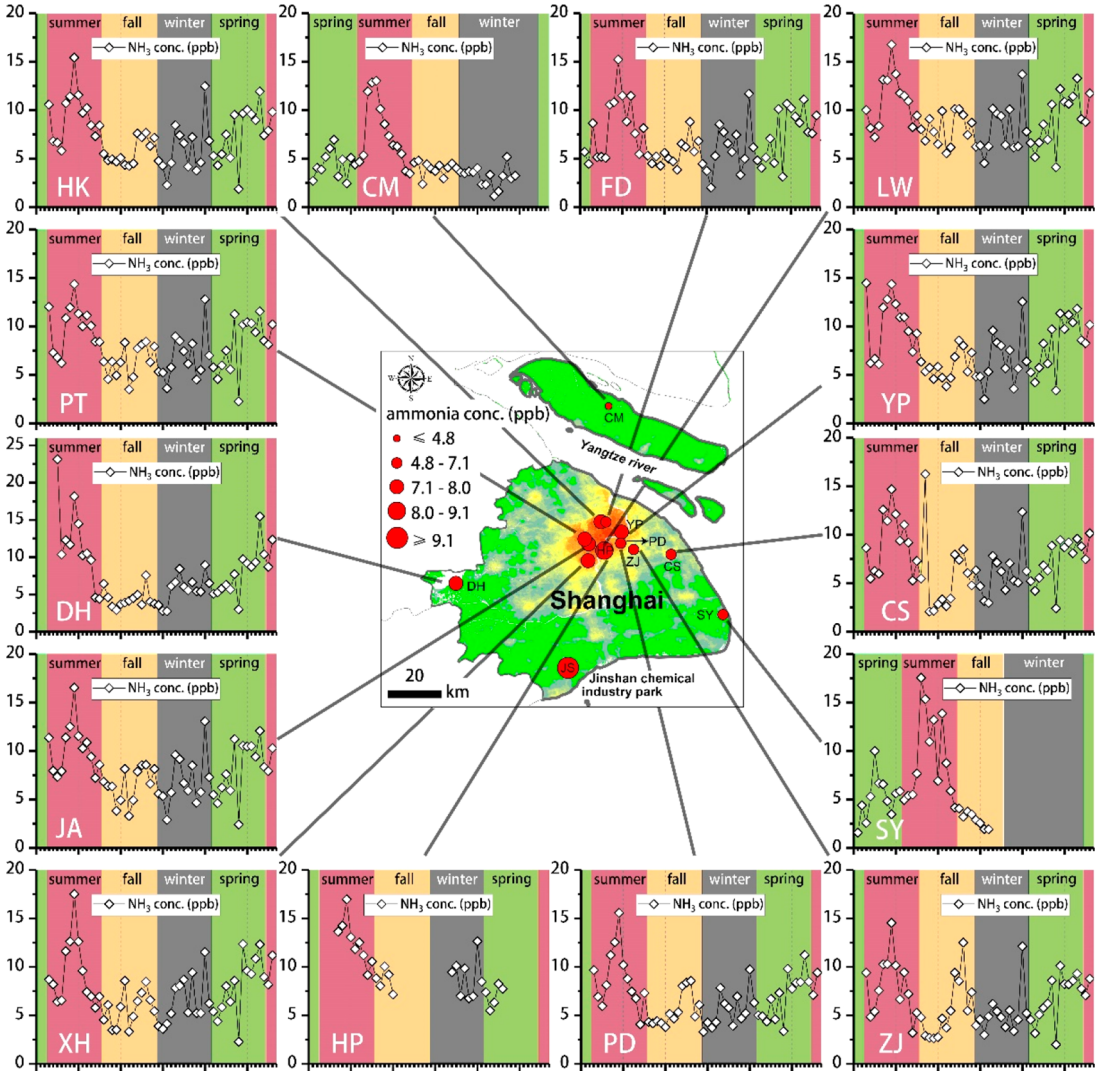

Figure 2. Sample-specific and group-averaged mixing ratios of ambient NH_3 measured with Ogawa passive samplers at 14 surface locations in Shanghai. Excepting the green color in the map (indicating rural areas), the color scheme is population density with the scale the same as that in Figure 1 (retrieved from worldpop.org.uk).

on-road traffic, NH_3 slip from coal-fired power plants), and urban waste volatilized sources (−37.8 ± 3.6‰; wastewater treatment, municipal solid waste, and human excreta).

2.6. Ancillary Information. Hourly meteorological parameters (MSO Weather Sensor, MetOne Instruments, U.S.A.; including wind direction, wind speed, relative humidity or RH, and temperature or *T*) in Shanghai were provided by the Shanghai Meteorological Bureau. Bivariate polar plots (BPP) were used to demonstrate how NH_3 concentrations vary with wind direction and wind speed in polar coordinates, an effective diagnostic technique for discriminating different source regions.[78−81] For creating BBPs, the open-source software "openair" in R was used.[79]

3. RESULTS AND DISCUSSION

3.1. Spatially Revolved Sampling Reveals Urban Areas As a Hot Spot of Atmospheric NH_3. A total of 702 duplicate passive samples were collected in this study. The passive sampling sites are divided into three types: urban (461 samples), suburban (108 samples), and rural (133 samples), based on local land use and economic activities. Weekly variations of atmospheric NH_3 concentrations at each observation site, and annual and seasonal average NH_3 concentrations (mean ±1 σ) among different sites and site categories are plotted in Figures 2 and 3, respectively. The observations from the Ogawa passive samplers are mainly used to illustrate spatial distributions rather than temporal variations of NH_3, due to their relatively coarse time resolution.

Taking the results of all weekly samples as a whole, atmospheric NH_3 concentrations in Shanghai range from 1.2 to 23.1 ppb, with a mean (±1σ) and median value of 7.3 (±3.1) and 6.8 ppb, respectively. Domestically, the annual average NH_3 concentrations in northern China (e.g., Beijing (23.5 ± 18.0 ppb)[82] and Xi'an (18.6 ppb on average)[83]) are much higher than our observations in Shanghai (Table 2). This can be partly explained by a higher soil pH in the North China Plain and the Guanzhong Plain where Beijing and Xi'an are located, respectively,[84] which promotes loss of NH_3.[85] Instead, the Yangtze River Delta region (including Shanghai) is dominated by acid soils of paddy fields.[86] Internationally, the average NH_3 level we measured in Shanghai is generally similar to observations in developed cities like Seoul in S. Korea[87] and Houston in the U.S.A.,[88] but much lower than in some cities in developing countries. This is particularly true when comparing

DOI: 10.1021/acs.est.8b05984
Environ. Sci. Technol. 2019, 53, 1822−1833

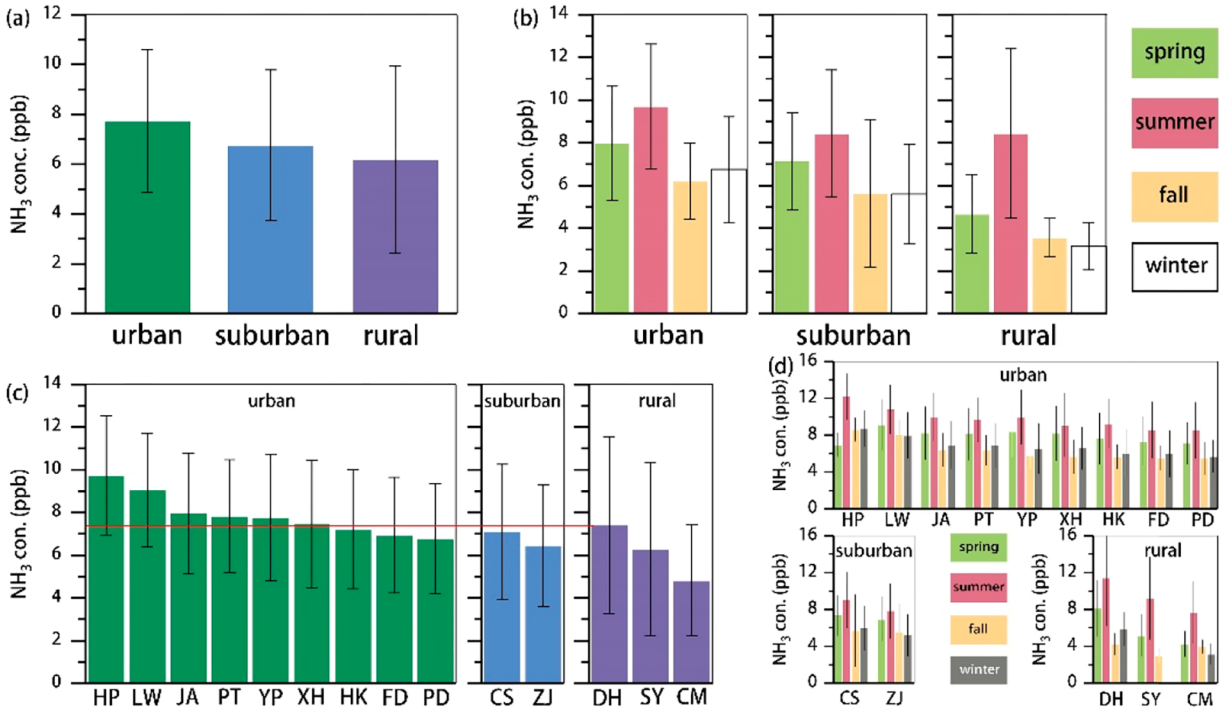

Figure 3. Comparison of the ambient NH_3 concentrations (mean $\pm 1\sigma$) among (a) different site types (urban/suburban/rural), (b) different seasons (spring/summer/fall/winter) within a specific site type, (c) different individual sites, and (d) different seasons (spring/summer/fall/winter) within a specific site.

Table 2. Comparison of Atmospheric NH_3 Concentrations (in ppb) between Urban and Suburban/Rural Areas in Different Regions

		average NH_3 concentration		
location	period	urban	suburban/rural	reference
Shanghai, CN	2014.5–2015.6	7.8	6.8/6.2	this study
Xi'an, CN	2006.4–2007.4	18.6	20.3	83
Beijing, CN	2007.1–2010.7	22.8	10.2	82
Hong Kong, CN	2003.10–2006.5	10.2	0.2	95
Delhi, IN	2012.10–2013.9	52.8	65.6	90
Rome, IT	2001.5–2002.3	5.3	3.5	96
Toronto, CA	2003.7–2011.9	2.3–3.0	0.1–4	97

with cities in South Asia (e.g., Delhi in India;[89] Table 2), where there is a lack of basic sanitation facilities (e.g., public flush toilets), and significant animal populations (such as cows) coexist with people in urban areas.[90] The high NH_3 concentrations measured at surface sites in South Asia are consistent with the spatial patterns determined from recent satellite remote sensing observations.[91,92] It is worth noting that from measurements in the Shanghai Jinshan chemical industry park (Figure 2), Wang et al.[93] showed a much higher NH_3 concentration (17.6 ± 9.5 ppb) with abrupt concentration changes on an hourly basis, a result of the strong influence of variable industrial emissions in the vicinity.

NH_3 levels were found to exhibit modest gradients across the study region, with mean NH_3 concentrations ranging from 4.8 (CM rural site) to 9.7 ppb (HP urban site) (Figures 2 and 3c). As discussed above, on a regional scale, NH_3 is mainly emitted from animal housing, manure storage, and land-spread manure, and to a smaller extent from mineral fertilizer application. The emission strengths of these sources are primarily determined by the activity of microbes, which is highly dependent on temperature.[94] Hence, rural areas with strong agricultural sources, are expected to experience increased emissions in summertime. Indeed, in our study, the average NH_3 concentrations in summer are higher than in other seasons for each land use category (Figure 3b) and site (Figure 3d), signifying the importance of volatilized NH_3 sources in the region (see discussion later). Somewhat surprisingly, however, the lowest average ambient NH_3 concentrations are found at rural sites such as CM (4.8 ± 2.6 ppb) and SY (6.3 ± 4.1 ppb), which are in active agricultural areas (Figure 3c). Although the average NH_3 concentration at the rural DH site (7.4 ± 4.1 ppb) is higher than 7 of the other 13 sites (Figure 3c), the overall average NH_3 concentration observed at urban sites (7.8 ± 2.9 ppb) is significantly higher than at suburban (6.8 ± 3.1 ppb, $p < 0.01$) and rural (6.2 ± 3.8 ppb, $p < 0.01$) sites (Figure 3a). In fact, urban enrichment of NH_3 in Shanghai is not unique. In Table 2 we compile previous studies in which urban NH_3 concentrations are comparable with or higher than suburban and rural NH_3 concentrations. In brief, our results demonstrate that urban areas, without agricultural activities, can also be an important source of NH_3 emissions.

DOI: 10.1021/acs.est.8b05984
Environ. Sci. Technol. 2019, 53, 1822–1833

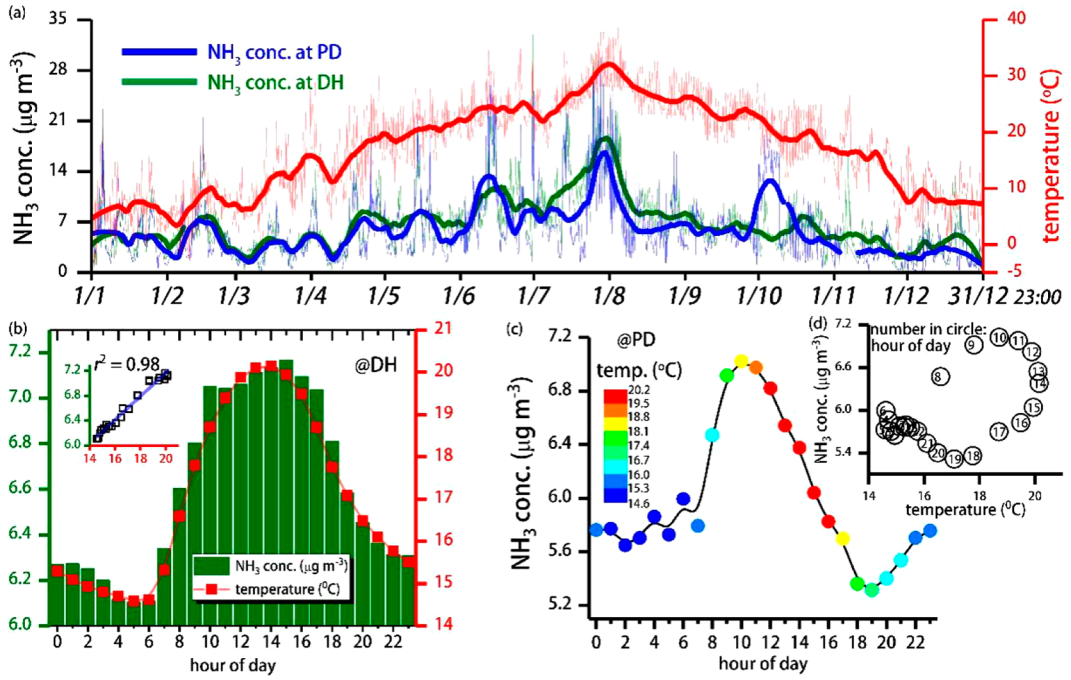

Figure 4. (a) Hourly variations of temperature (red) in Shanghai and NH_3 concentrations at the PD urban site (blue) and DH rural site (green), along with 500-point Savitzky-Golay smoothed records from 1 January to 31 December 2015. (b) Diurnal variation of NH_3 concentration and temperature and their correlation at DH rural site in 2015. (c) Diurnal variation of NH_3 concentration (colored by temperature) at the urban PD site in 2015. (d) Scatter plot of diurnal temperature and NH_3 concentration at the urban PD site in 2015.

Temperature is the key driver of NH_3 emissions from volatility-driven sources; observations of NH_3 volatilization by Sommer et al.[98] found that NH_3 emissions after 6 h of surface applied cattle slurry were exponentially related to temperature ($r^2 > 0.80$). As shown in Figures 2 and 3d, the average NH_3 concentrations are higher in summer and lower in winter. This is particularly true at rural sites, consistent with dominant, temperature-sensitive emission of NH_3 from agricultural sources like livestock waste and fertilizer application. There are also other temperature-sensitive sources in urban areas like wastewater, household garbage, golf turf, and human excreta; the latter two are often overlooked but important NH_3 sources in urban China.[44,99] Although still recognized as a luxury sport by most Chinese people, golf is increasingly popular.[44] In contrast to Western industrialized countries, golf courses in China tend to operate in urban areas, which are closer to the affluent consumer.[44] Also different from other developed countries, human excreta in urban China is typically first stored in a three-grille septic tank beneath the building.[61] After a series of anaerobic decomposition processes, a substantial amount of odors (including NH_3) will be generated and emitted through a ceiling duct.[61]

From a climate perspective, differences in temperature and other meteorological parameters (e.g., precipitation, wind speed, planetary boundary layer) over the Shanghai region are minor.[36] Interestingly, the lowest NH_3 concentrations at urban Shanghai sites were not observed in the winter, while the NH_3 difference between summer and winter is much lower at urban sites than at rural sites in our data set (Figure 3). These observations suggest that there may be some other temperature-independent NH_3 sources present in urban areas.

3.2. Significant Influences of Nonagricultural NH_3 Emissions in the Urban Atmosphere. The analysis of weekly NH_3 samples collected from our network of sites spanning various land use categories indicates that the enhancement of atmospheric NH_3 at urban sites reflects a mix of agricultural and nonagricultural NH_3 emissions. To further explore and compare the influences of various NH_3 sources on ambient NH_3 in urban and rural atmospheres, we can examine the year-round, hourly observations of NH_3 at the urban PD and rural DH sites (Figure 1). By combining hourly concentration, wind speed, and wind direction measurements, bivariate polar plots (BPP) can be constructed to identify source regions of near-ground pollutants like NH_3, an approach that has proven to be a more suitable tool than back trajectory-based methods.[78,80,81]

As illustrated in Figure 4a, there are large temporal variations in NH_3 concentrations at the urban PD and rural DH site, with their hourly NH_3 concentrations ranging from 0.1 to 36.4 $\mu g\ m^{-3}$ (mean $\pm$ 1σ = 5.9 $\pm$ 4.5 $\mu g\ m^{-3}$; median = 4.8 $\mu g\ m^{-3}$; n = 7897; 90.1% data availability) and 0.1 to 33.0 $\mu g\ m^{-3}$ (mean $\pm$ 1σ = 6.6 $\pm$ 4.1 $\mu g\ m^{-3}$; median = 5.9 $\mu g\ m^{-3}$; n = 8204; 93.7% data availability), respectively. The NH_3 concentration spikes at both sites are concentrated in summer (June, July, and August), and their smoothed trends are generally consistent with the variation of temperature. These findings suggest that volatilized NH_3 emissions are a regionally important NH_3 source in Shanghai.

Also included in Figure 4 are, to help further identify specific sources, the diurnal profiles of NH_3 and temperature at DH and PD. At the rural DH site, diurnal variations of NH_3 concentrations are highly correlated with temperature (r^2 = 0.98, $p < 0.01$; Figure 4b), indicating the predominant role of volatilization-related NH_3 sources in rural areas. In eastern China (including Shanghai), agricultural sources (livestock feeding and N-fertilizer application) make up nearly 90% of the total NH_3 emissions.[22] Indeed, in Figure 5a, the BPP analysis shows that high NH_3 concentrations at DH are associated with

DOI: 10.1021/acs.est.8b05984
Environ. Sci. Technol. 2019, 53, 1822−1833

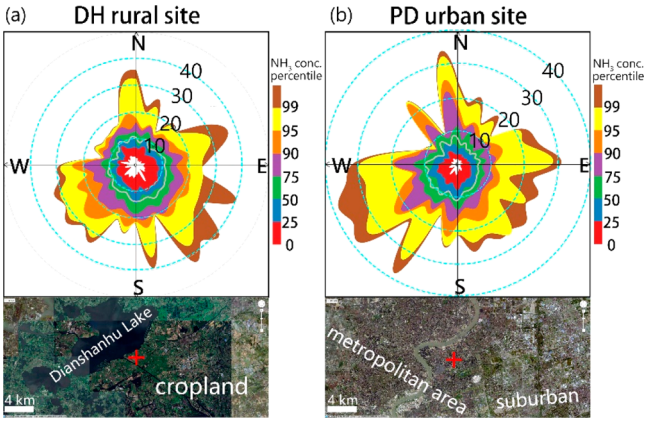

Figure 5. Bivariate polar plots (BPP) of the percentiles of NH_3 concentrations at (a) rural DH site and (b) urban PD site. The natural-color satellite images below are the land use maps corresponding to each site.

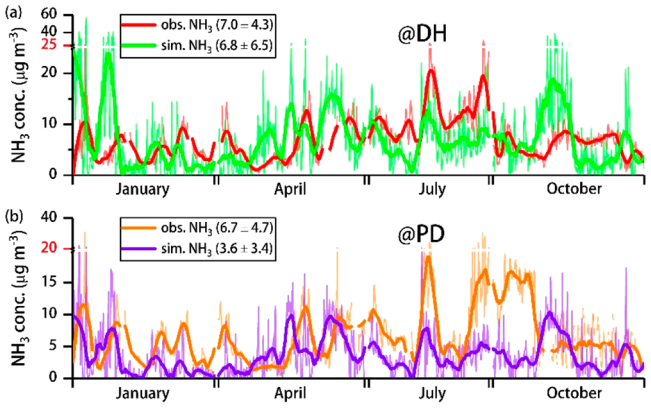

Figure 6. Comparison of hourly observed and simulated NH_3 concentrations at (a) DH rural site and (b) PD urban site.

air flows from the southwest and the southeast but infrequently from the northwest. This can be explained by the large lake Dianshanhu in the northwest, which has negligible NH_3 emission potential.[44,45] The south and east side of the lake is covered by intensive cultivation areas, with modern agriculture facilities.[61] The areas to the southeast of the sampling site have been described as the "backyard garden" of Shanghai, renowned for its idyllic scene, and are a regional hot spot of agricultural NH_3 emissions.[22,61]

At the urban PD site, however, distinctly different pictures of the diurnal profiles of NH_3 and temperature are observed (see Figure 4c and d), suggesting a complex mix of NH_3 source contributions. Specifically, there is no correlation between NH_3 concentration and temperature on a diurnal basis (Figure 4d). The average concentrations of NH_3 show a well-marked bimodal pattern, which is generally similar to the diurnal evolution of urban traffic flow in Shanghai.[17] Previous observations have also shown coincident enhancements of NH_3 and carbon monoxide (CO) in the Shanghai urban atmosphere.[36] Following a stable period of NH_3 concentrations between 22:00 and 5:00 (5.7 ± 0.1 $\mu g\ m^{-3}$), the maximum NH_3 concentration occurs in the morning rush hour (7.0 $\mu g\ m^{-3}$, 10:00), 22% higher than the overnight level. In Figure 5b, the Shanghai metropolitan area to the southwest and the suburban Pudong District to the southeast are indicated as two prominent NH_3 source regions. The metropolitan area is densely populated with intense traffic, representing an important source region of nonagricultural NH_3 emissions (including vehicles). The suburban Pudong District, for long stretches, serves as the primary animal feeding operation region in Eastern China, where almost all livestock farms are focused on hog rearing.[61]

To further examine the NH_3 emissions potential from vehicles, we measured NH_3 concentrations emitted from tailpipe exhaust of 19 different vehicles equipped with TWCs. The average NH_3 concentration of the total 57 samples (10.2 ppm) is 4 orders of magnitude higher than the ambient NH_3 concentrations. Considering the huge automobile inventory in Shanghai (nearly 3.3 million in 2015),[36] our study strongly suggests that on-road traffic is an important NH_3 source in the urban atmosphere.

3.3. NH_3 from Nonagricultural Rival Agricultural Emissions in the Urban Atmosphere. Figure 6 compares model simulations and measurements of hourly NH_3 concentration at the rural DH and urban PD sites. The average measured and predicted NH_3 concentrations at DH are similar, although the variability in the model predictions is much larger than the observations, perhaps reflecting the coarse time resolution of the emission inventory used. It is noteworthy that the average NH_3 concentration at the rural DH site is accurate without any nonagricultural NH_3 emissions being included in the model, consistent with our conclusion above that agricultural activities are the predominant NH_3 source in rural areas. At the urban PD site, the simulation with only agricultural NH_3 emissions yields an average predicted NH_3 concentration (3.6 $\mu g\ m^{-3}$) that is 47% lower than the average measured concentration (6.7 $\mu g\ m^{-3}$), suggesting that (nonsimulated) emissions from nonagricultural activities are important contributors to urban NH_3. Although other factors could contribute to under-prediction of urban NH_3 (e.g., incorrectly modeled transport from rural agricultural sources or overestimation of the rate of dry deposition of NH_3 emitted by agricultural sources), past studies suggest that ambient NH_3 concentrations most strongly depend on NH_3 emissions rather than atmospheric processes,[100,101] suggesting that ignoring nonagricultural NH_3 emissions is likely one of the most important reasons for the low concentration model bias at PD.

A quantitative and accurate assessment of NH_3 sources in the urban atmosphere is difficult to obtain solely using the approach described above. Below we demonstrate the complementary use of N isotopes to better constrain NH_3 source contributions at the PD site. Although there is generally not a compelling need to differentiate agricultural vs nonagricultural emissions contributions in rural areas, the relative contributions of N-fertilizer application and livestock feeding are certainly of interest and isotopic signatures are also used to constrain these source contributions at the rural DH site.

Isotope-based source apportionment of atmospheric NH_3 requires a well-established pool of NH_3 isotopic source signatures ($\delta^{15}N\text{-}NH_3$) to allow a separation of different sources. From a total of 44 NH_3 source samples in our previous study,[65] we have established a pool of isotopic signatures for the major NH_3 emission sources in Eastern China (Table 1). The NH_3 concentrations and $\delta^{15}N$ values of these samples ranged from 33 to 6211 $\mu g\ m^{-3}$ and −52.0 to −9.6‰, respectively. Recently, NH_3 slip from coal-fired power plants equipped with selective catalytic reduction (SCR) technology was reported as an important source of NH_3; thus,

DOI: 10.1021/acs.est.8b05984
Environ. Sci. Technol. 2019, 53, 1822−1833

its isotopic signature, as reported by Felix et al.,[76] is also considered in this study. Table 1 shows that these NH_3 sources can be clearly classified into four categories by specific isotope signatures: NH_3 emitted from combustion-related sources has relatively high $\delta^{15}N$ values, allowing them to be distinguished from NH_3 emitted from volatilization processes. The $\delta^{15}N$ values (mean $\pm 1\sigma$) of the Shanghai urban PD site environmental samples collected in July and August of 2015 were $-31.72 \pm 3.36‰$ (ranging from $-36.01‰$ to $-25.40‰$, n = 10), close to the $\delta^{15}N$-NH_3 values observed in Beijing ($-34.0‰$ to $-27.2‰$, n = 4; a period without strict air quality control measures)[65] and higher than at the rural DH site ($-41.03‰$, $-36.53‰$), suggesting a stronger influence of combustion-related sources in the urban atmosphere.

At the rural DH site, our earlier analysis demonstrated that rural NH_3 concentrations can be solely attributed to agricultural NH_3 emissions, i.e., livestock breeding (LB) and fertilizer application (FA). Therefore, the isotopic signatures of two sources, i.e., LB and FA, are used as input into the SIAR Bayesian mixing model. The results suggest that on average, LB and FA contribute 51.9% and 48.1% to the measured NH_3 concentrations, respectively (not shown). From the perspective of the emissions inventory, the NH_3 emissions from LB and FA contribute 48% and 40% to the total in Eastern China, respectively,[22] in general agreement with our results.

At the PD urban site with its more complex NH_3 sources, normal distributions and variation ranges (within 5 and 95 percentiles) of the relative contribution fractions of each source to the ambient NH_3 concentrations were estimated and are depicted in Figure 7. As a reminder, the availability of only

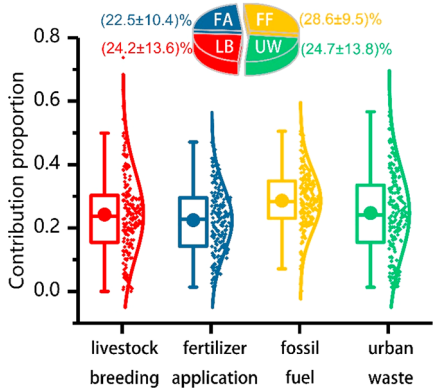

Figure 7. Isotope-based source apportionment of atmospheric NH_3 at PD urban site with the normal distribution and variation range (within 5 and 95 percentiles).

a single isotopic tracer vs four hypothesized source types, means that there is no unique solution for the system;[102,103] however, we can identify all possible sets of source contributions that reproduce the observed isotopic signature. The utility of this analysis will depend, to a large extent, on how narrow the source contribution ranges are for each source. In our analysis, fossil fuel-related sources (FF) and fertilizer application (FA) have relatively low variation ranges (Figure 7), indicating that they are better constrained than livestock breeding (LB; -31.7% to -27.1%) and urban waste volatilized (UW; -41.9% to -29.9%) sources. This is because the isotopic signatures of LB and UW are distributed in the middle of the source pool, where their contributions to the $\delta^{15}N$ values of the ambient NH_3 ($-36.01‰$ to $-25.40‰$) are less well constrained. The pie chart in Figure 7 illustrates the overall mean contribution proportions. While estimates of the mean values are inherently uncertain,[102] the four source contribution distribution estimates strongly suggest that all four source types make substantial contributions to the NH_3 concentrations measured at the urban PD site. Further, this isotopic analysis lends further confidence to our earlier conclusion from the WRF-CMAQ model vs observations comparison that nonagricultural sources rival agricultural sources in terms of contributing to ambient NH_3 in the urban atmosphere.

Fossil fuel-related sources are identified as an important contributor to ambient NH_3 concentrations at PD. Although NH_3 emissions from coal and biomass burning are observed,[26,30] they are not comparable with the magnitude of vehicular NH_3 emissions and NH_3 slip from SCR-equipped coal-fired power plant (CFPP).[30,37] Recently, a five-year plan was introduced in China to slash coal consumption from CFPP and household sectors.[77] For example, in 2016, all CFPPs in Beijing were replaced with gas-fired power plants to cut pollution.[77] The replacement by the four gas-fired power plants will help cut emissions by 10 000 tons of SO_2 and 19 000 tons of NO annually.[77] Although NH_3 slip is a common issue with SCR technology used in CFPP for the removal of NO, the mass concentration of NH_3 (typically 3−5 mg NH_3 m^{-3}) in flue gases is two or 3 orders of magnitude smaller than that of NO_x.[77] Therefore, we suspect that the share of NH_3 emissions from SCR-equipped CFPP in urban areas is relatively small and will decrease continuously in China. In the U.S.A., it is estimated that 5% of the national NH_3 emissions are derived from motor vehicles, while this figure is estimated at 12% for the U.K., with almost all the remaining NH_3 coming from agricultural processes.[45] In China, all new light-duty vehicles were required to install TWC since 2009.[44] In Table S1, we have provided direct evidence that TWC-equipped vehicles are an important urban source of NH_3. Thus, expanding vehicular NH_3 emissions in urban China can be expected. Indeed, the average contribution of fossil fuel-related sources derived from the Bayesian isotopic mixing model (28.6%) is close to the share of on-road traffic (22.3%), we estimated the above based on NH_3 concentration analysis at PD. This suggests that fossil fuel-derived NH_3 concentrations in urban Shanghai are primarily emitted from on-road traffic.

4. IMPLICATIONS AND OUTLOOK

The present study outlines a framework to integrate NH_3 concentration measurements, atmospheric transport modeling, and isotope-based source apportionment to address a long-standing and ongoing controversy regarding sources of NH_3 in the urban atmosphere. We validate the feasibility of this approach by application to the Yangtze River Delta region, with a focus on the megacity of Shanghai. Results from a Shanghai passive NH_3 monitoring network (14 locations) reveal a broadly homogeneous distribution of NH_3 concentrations throughout the region and pinpoint urban areas as a hot spot of NH_3. The acquired data also provide a baseline toward tracking future NH_3 emissions changes. The year-round online measurements of NH_3 at an urban and rural site, and a comparison against concentrations simulated by the WRF-CMAQ chemical transport model, demonstrate that NH_3 in the rural atmosphere can be attributed to emissions from agricultural sources, while there is a significant contribution from nonagricultural NH_3 emissions, particularly vehicular NH_3 emissions, in the urban atmosphere. Isotope-

DOI: 10.1021/acs.est.8b05984
Environ. Sci. Technol. 2019, 53, 1822−1833

based source apportionment of NH_3 in the urban atmosphere further indicates that nonagricultural NH_3 emissions, missing from the current emission inventory, could well rival agricultural NH_3 emissions in terms of contributing to ambient NH_3.

Given the central role of NH_3 in the formation of secondary inorganic aerosols and resulting haze, our results are of critical importance for China as it seeks to curb its severe $PM_{2.5}$ pollution. Additional useful investigative steps could include: (1) sensitivity analyses with the WRF-CMAQ model to further diagnose the importance of nonagricultural NH_3 emissions through developing a gridded nonagricultural NH_3 emissions inventory with high time resolution; (2) collecting NH_3 and aerosol NH_4^+ for simultaneously determining the mass concentrations and isotopic compositions at high time resolution; and (3) improving the pool of isotopic source signatures of NH_3 from fuel-related sources.

■ ASSOCIATED CONTENT

Supporting Information

The Supporting Information is available free of charge on the ACS Publications website at DOI: 10.1021/acs.est.8b05984.

Figure S1, A summary of the average monthly temperature and precipitation in Shanghai; Text S1, details regarding the method used to collect vehicle-emitted NH_3; and Text S2, model frame and computing methods of the SIAR (Stable Isotope Analysis in R) (PDF)

■ AUTHOR INFORMATION

Corresponding Authors

*E-mail: dryanlinzhang@outlook.com (Y.Z.).
*E-mail: congruideng@fudan.edu.cn (C.D.).

ORCID

Yunhua Chang: 0000-0002-1622-5330
Yanlin Zhang: 0000-0002-8722-8635

Author Contributions

#These authors contributed equally to this work.

Notes

The authors declare no competing financial interest.

■ ACKNOWLEDGMENTS

This study was supported by the National Key R&D Program of China (Grant no. 2017YFC0210101), National Natural Science Foundation of China (Grant Nos. 41705100, 91644103), the Provincial Natural Science Foundation of Jiangsu (Grant nos. BK20180040, BK20170946), and University Science Research Project of Jiangsu Province (17KJB170011). Anthony J. Dore thanks the support of the SUNRISE programme funded by the Natural Environment Research Council (NERC) as part of a National Capability Long-Term Science - Official Development Assistance Award.

■ REFERENCES

(1) Wang, Y.; Zhang, Q. Q.; He, K.; Zhang, Q.; Chai, L. Sulfate-nitrate-ammonium aerosols over China: Response to 2000−2015 emission changes of sulfur dioxide, nitrogen oxides, and ammonia. *Atmos. Chem. Phys.* **2013**, *13* (5), 2635−2652.

(2) Walker, J. M.; Philip, S.; Martin, R. V.; Seinfeld, J. H. Simulation of nitrate, sulfate, and ammonium aerosols over the United States. *Atmos. Chem. Phys.* **2012**, *12* (22), 11213−11227.

(3) Zhang, X. Y.; Wang, Y. Q.; Niu, T.; Zhang, X. C.; Gong, S. L.; Zhang, Y. M.; Sun, J. Y. Atmospheric aerosol compositions in China: Spatial/temporal variability, chemical signature, regional haze distribution and comparisons with global aerosols. *Atmos. Chem. Phys.* **2012**, *12* (2), 779−799.

(4) Yang, F.; Tan, J.; Zhao, Q.; Du, Z.; He, K.; Ma, Y.; Duan, F.; Chen, G.; Zhao, Q. Characteristics of $PM_{2.5}$ speciation in representative megacities and across China. *Atmos. Chem. Phys.* **2011**, *11* (11), 5207−5219.

(5) Huang, R. J.; Zhang, Y.; Bozzetti, C.; Ho, K. F.; Cao, J. J.; Han, Y.; Daellenbach, K. R.; Slowik, J. G.; Platt, S. M.; Canonaco, F.; Zotter, P.; Wolf, R.; Pieber, S. M.; Bruns, E. A.; Crippa, M.; Ciarelli, G.; Piazzalunga, A.; Schwikowski, M.; Abbaszade, G.; Schnelle-Kreis, J.; Zimmermann, R.; An, Z.; Szidat, S.; Baltensperger, U.; El Haddad, I.; Prevot, A. S. High secondary aerosol contribution to particulate pollution during haze events in China. *Nature* **2014**, *514* (7521), 218−222.

(6) Paulot, F.; Jacob, D. J. Hidden cost of US agricultural exports: Particulate matter from ammonia emissions. *Environ. Sci. Technol.* **2014**, *48* (2), 903−908.

(7) Pinder, R. W.; Adams, P. J.; Pandis, S. N. Ammonia emission controls as a cost-effective strategy for reducing atmospheric particulate matter in the eastern United States. *Environ. Sci. Technol.* **2007**, *41* (2), 380−386.

(8) Heo, J.; Adams, P. J.; Gao, H. O. Public health costs of primary $PM_{2.5}$ and inorganic $PM_{2.5}$ precursor emissions in the United States. *Environ. Sci. Technol.* **2016**, *50* (11), 6061−6070.

(9) Brunekreef, B.; Harrison, R. M.; Künzli, N.; Querol, X.; Sutton, M. A.; Heederik, D. J. J.; Sigsgaard, T. Reducing the health effect of particles from agriculture. *Lancet Respir. Med.* **2015**, *3* (11), 831−832.

(10) Lee, C. J.; Martin, R. V.; Henze, D. K.; Brauer, M.; Cohen, A.; Donkelaar, A. V. Response of global particulate-matter-related mortality to changes in local precursor emissions. *Environ. Sci. Technol.* **2015**, *49* (7), 4335−4344.

(11) Warner, J. X.; Dickerson, R. R.; Wei, Z.; Strow, L. L.; Wang, Y.; Liang, Q. Increased atmospheric ammonia over the world's major agricultural areas detected from space. *Geophys. Res. Lett.* **2017**, *44* (6), 2875−2884.

(12) Liu, L.; Zhang, X.; Xu, W.; Liu, X.; Li, Y.; Lu, X.; Zhang, Y.; Zhang, W. Temporal characteristics of atmospheric ammonia and nitrogen dioxide over China based on emission data, satellite observations and atmospheric transport modeling since 1980. *Atmos. Chem. Phys.* **2017**, *17* (15), 9365−9378.

(13) Kang, Y.; Liu, M.; Song, Y.; Huang, X.; Yao, H.; Cai, X.; Zhang, H.; Kang, L.; Liu, X.; Yan, X.; He, H.; Zhang, Q.; Shao, M.; Zhu, T. High-resolution ammonia emissions inventories in China from 1980 to 2012. *Atmos. Chem. Phys.* **2016**, *16* (4), 2043−2058.

(14) Aneja, V. P.; Schlesinger, W. H.; Erisman, J. W. Farming pollution. *Nat. Geosci.* **2008**, *1* (7), 409−411.

(15) Reis, S.; Pinder, R.; Zhang, M.; Lijie, G.; Sutton, M. Reactive nitrogen in atmospheric emission inventories. *Atmos. Chem. Phys.* **2009**, *9* (19), 7657−7677.

(16) Van Damme, M.; Wichink Kruit, R. J.; Schaap, M.; Clarisse, L.; Clerbaux, C.; Coheur, P.; Dammers, E.; Dolman, A. J.; Erisman, J. W. Evaluating 4 years of atmospheric ammonia (NH_3) over Europe using IASI satellite observations and LOTOS-EUROS model results. *J. Geophys. Res.* **2014**, *119* (15), 9549−9566.

(17) Xu, P.; Liao, Y. J.; Lin, Y. H.; Zhao, C. X.; Yan, C. H.; Cao, M. N.; Wang, G. S.; Luan, S. J. High-resolution inventory of ammonia emissions from agricultural fertilizer in China from 1978 to 2008. *Atmos. Chem. Phys.* **2016**, *16* (3), 1207−1218.

(18) Bouwman, A. F.; Lee, D. S.; Asman, W. A. H.; Dentener, F. J.; Van Der Hoek, K. W.; Olivier, J. G. J. A global high-resolution emission inventory for ammonia. *Global Biogeochem. Cy.* **1997**, *11* (4), 561−587.

(19) Heald, C. L.; Collett, J., Jr; Lee, T.; Benedict, K.; Schwandner, F.; Li, Y.; Clarisse, L.; Hurtmans, D.; Van Damme, M.; Clerbaux, C.; et al. Atmospheric ammonia and particulate inorganic nitrogen over the United States. *Atmos. Chem. Phys.* **2012**, *12* (21), 10295−10312.

DOI: 10.1021/acs.est.8b05984
Environ. Sci. Technol. 2019, 53, 1822−1833

(20) Zhang, L.; Chen, Y.; Zhao, Y.; Henze, D. K.; Zhu, L.; Song, Y.; Paulot, F.; Liu, X.; Pan, Y.; Lin, Y.; Huang, B. Agricultural ammonia emissions in China: Reconciling bottom-up and top-down estimates. *Atmos. Chem. Phys.* **2018**, *18* (1), 339−355.
(21) Balasubramanian, S.; Koloutsou-Vakakis, S.; McFarland, D. M.; Rood, M. J. Reconsidering emissions of ammonia from chemical fertilizer usage in Midwest USA. *J. Geophys. Res.* **2015**, *120* (12), 6232−6246.
(22) Huang, C.; Chen, C. H.; Li, L.; Cheng, Z.; Wang, H. L.; Huang, H. Y.; Streets, D. G.; Wang, Y. J.; Zhang, G. F.; Chen, Y. R. Emission inventory of anthropogenic air pollutants and VOC species in the Yangtze River Delta region, China. *Atmos. Chem. Phys.* **2011**, *11* (9), 4105−4120.
(23) Aneja, V. P.; Schlesinger, W. H.; Erisman, J. W. Effects of agriculture upon the air quality and climate: Research, policy, and regulations. *Environ. Sci. Technol.* **2009**, *43* (12), 4234−4240.
(24) Wang, S.; Xing, J.; Jang, C.; Zhu, Y.; Fu, J. S.; Hao, J. Impact assessment of ammonia emissions on inorganic aerosols in East China using response surface modeling technique. *Environ. Sci. Technol.* **2011**, *45* (21), 9293−300.
(25) Zhang, C.; Geng, X.; Wang, H.; Zhou, L.; Wang, B. Emission factor for atmospheric ammonia from a typical municipal wastewater treatment plant in South China. *Environ. Pollut.* **2017**, *220*, 963−970.
(26) Li, Q.; Jiang, J.; Cai, S.; Zhou, W.; Wang, S.; Duan, L.; Hao, J. Gaseous ammonia emissions from coal and biomass combustion in household stoves with different combustion efficiencies. *Environ. Sci. Technol. Lett.* **2016**, *3* (3), 98−103.
(27) Reche, C.; Viana, M.; Pandolfi, M.; Alastuey, A.; Moreno, T.; Amato, F.; Ripoll, A.; Querol, X. Urban NH_3 levels and sources in a Mediterranean environment. *Atmos. Environ.* **2012**, *57*, 153−164.
(28) Suarez-Bertoa, R.; Zardini, A.; Astorga, C. Ammonia exhaust emissions from spark ignition vehicles over the new European driving cycle. *Atmos. Environ.* **2014**, *97*, 43−53.
(29) Teng, X.; Hu, Q.; Zhang, L.; Qi, J.; Shi, J.; Xie, H.; Gao, H.; Yao, X. Identification of major sources of atmospheric NH_3 in an urban environment in Northern China during wintertime. *Environ. Sci. Technol.* **2017**, *51* (12), 6839−6848.
(30) Meng, W.; Zhong, Q.; Yun, X.; Zhu, X.; Huang, T.; Shen, H.; Chen, Y.; Chen, H.; Zhou, F.; Liu, J.; Wang, X.; Zeng, E. Y.; Tao, S. Improvement of a global high-resolution ammonia emission inventory for combustion and industrial sources with new data from the residential and transportation sectors. *Environ. Sci. Technol.* **2017**, *51* (5), 2821−2829.
(31) Pierson, W. R.; Brachaczek, W. W. Emissions of ammonia and amines from vehicles on the road. *Environ. Sci. Technol.* **1983**, *17* (12), 757−760.
(32) Heeb, N. V.; Forss, A. M.; Brühlmann, S.; Lüscher, R.; Saxer, C. J.; Hug, P. Three-way catalyst-induced formation of ammonia—velocity-and acceleration-dependent emission factors. *Atmos. Environ.* **2006**, *40* (31), 5986−5997.
(33) Fenn, M. E.; Bytnerowicz, A.; Schilling, S. L.; Vallano, D. M.; Zavaleta, E. S.; Weiss, S. B.; Morozumi, C.; Geiser, L. H.; Hanks, K. On-road emissions of ammonia: an underappreciated source of atmospheric nitrogen deposition. *Sci. Total Environ.* **2018**, *625*, 909−919.
(34) Kean, A. J.; Harley, R. A.; Littlejohn, D.; Kendall, G. R. On-road measurement of ammonia and other motor vehicle exhaust emissions. *Environ. Sci. Technol.* **2000**, *34* (17), 3535−3539.
(35) Zhang, Y.; Tang, A.; Wang, D.; Wang, Q.; Benedict, K.; Zhang, L.; Liu, D.; Li, Y.; Collett, J. L., Jr.; Sun, Y.; Liu, X. The vertical variability of ammonia in urban Beijing, China. *Atmos. Chem. Phys.* **2018**, *18*, 16385−16398.
(36) Chang, Y.; Zou, Z.; Deng, C.; Huang, K.; Collett, J. L.; Lin, J.; Zhuang, G. The importance of vehicle emissions as a source of atmospheric ammonia in the megacity of Shanghai. *Atmos. Chem. Phys.* **2016**, *16* (5), 3577−3594.
(37) Sun, K.; Tao, L.; Miller, D. J.; Pan, D.; Golston, L. M.; Zondlo, M. A.; Griffin, R. J.; Wallace, H. W.; Leong, Y. J.; Yang, M. M.; Zhang, Y.; Mauzerall, D. L.; Zhu, T. Vehicle emissions as an important urban ammonia source in the United States and China. *Environ. Sci. Technol.* **2017**, *51* (4), 2472−2481.
(38) Fraser, M. P.; Cass, G. R. Detection of excess ammonia emissions from in-use vehicles and the implications for fine particle control. *Environ. Sci. Technol.* **1998**, *32* (8), 1053−1057.
(39) Huai, T.; Durbin, T. D.; Miller, J. W.; Pisano, J. T.; Sauer, C. G.; Rhee, S. H.; Norbeck, J. M. Investigation of NH_3 emissions from new technology vehicles as a function of vehicle operating conditions. *Environ. Sci. Technol.* **2003**, *37* (21), 4841−4847.
(40) Liu, T.; Wang, X.; Wang, B.; Ding, X.; Deng, W.; Lü, S.; Zhang, Y. Emission factor of ammonia (NH_3) from on-road vehicles in China: Tunnel tests in urban Guangzhou. *Environ. Res. Lett.* **2014**, *9* (6), 064027.
(41) Kean, A. J.; Littlejohn, D.; Ban-Weiss, G. A.; Harley, R. A.; Kirchstetter, T. W.; Lunden, M. M. Trends in on-road vehicle emissions of ammonia. *Atmos. Environ.* **2009**, *43* (8), 1565−1570.
(42) Nowak, J. B.; Huey, L. G.; Russell, A. G.; Tian, D.; Neuman, J. A.; Orsini, D.; Sjostedt, S. J.; Sullivan, A. P.; Tanner, D. J.; Weber, R. J.; Nenes, A.; Edgerton, E.; Fehsenfeld, F. C., Analysis of urban gas phase ammonia measurements from the 2002 Atlanta Aerosol Nucleation and Real-Time Characterization Experiment (ANARChE). *J. Geophys. Res.* **2006**, *111*, (D17), DOI: 10.1029/2006JD007113.
(43) Yao, X.; Hu, Q.; Zhang, L.; Evans, G. J.; Godri, K. J.; Ng, A. C. Is vehicular emission a significant contributor to ammonia in the urban atmosphere? *Atmos. Environ.* **2013**, *80*, 499−506.
(44) Chang, Y. H. Non-agricultural ammonia emissions in urban China. *Atmos. Chem. Phys. Discuss.* **2014**, *14* (6), 8495−8531.
(45) Sutton, M. A.; Dragosits, U.; Tang, Y.; Fowler, D. Ammonia emissions from non-agricultural sources in the UK. *Atmos. Environ.* **2000**, *34* (6), 855−869.
(46) Battye, W.; Aneja, V. P.; Roelle, P. A. Evaluation and improvement of ammonia emissions inventories. *Atmos. Environ.* **2003**, *37* (27), 3873−3883.
(47) Li, Y.; Thompson, T. M.; Van Damme, M.; Chen, X.; Benedict, K. B.; Shao, Y.; Day, D.; Boris, A.; Sullivan, A. P.; Ham, J.; Whitburn, S.; Clarisse, L.; Coheur, P. F.; Collett, J. L., Jr Temporal and spatial variability of ammonia in urban and agricultural regions of northern Colorado, United States. *Atmos. Chem. Phys.* **2017**, *17* (10), 6197−6213.
(48) Puchalski, M. A.; Sather, M. E.; Walker, J. T.; Lehmann, C. M.; Gay, D. A.; Mathew, J.; Robarge, W. P. Passive ammonia monitoring in the United States: Comparing three different sampling devices. *J. Environ. Monit.* **2011**, *13* (11), 3156−67.
(49) Li, Y.; Schichtel, B. A.; Walker, J. T.; Schwede, D. B.; Chen, X.; Lehmann, C. M. B.; Puchalski, M. A.; Gay, D. A.; Collett, J. L. Increasing importance of deposition of reduced nitrogen in the United States. *Proc. Natl. Acad. Sci. U. S. A.* **2016**, *113* (21), 5874−5879.
(50) Liu, X.; Zhang, Y.; Han, W.; Tang, A.; Shen, J.; Cui, Z.; Vitousek, P.; Erisman, J. W.; Goulding, K.; Christie, P.; Fangmeier, A.; Zhang, F. Enhanced nitrogen deposition over China. *Nature* **2013**, *494*, 459−463.
(51) Lu, C.; Tian, H. Half-century nitrogen deposition increase across China: a gridded time-series data set for regional environmental assessments. *Atmos. Environ.* **2014**, *97*, 68−74.
(52) Lü, C.; Tian, H. Spatial and temporal patterns of nitrogen deposition in China: Synthesis of observational data. *J. Geophys. Res.* **2007**, *112*, (D22), DOI: 10.1029/2006JD007990.
(53) Jia, Y.; Yu, G.; He, N.; Zhan, X.; Fang, H.; Sheng, W.; Zuo, Y.; Zhang, D.; Wang, Q. Spatial and decadal variations in inorganic nitrogen wet deposition in China induced by human activity. *Sci. Rep.* **2015**, *4*, 3763.
(54) Liu, J.; Kuang, W.; Zhang, Z.; Xu, X.; Qin, Y.; Ning, J.; Zhou, W.; Zhang, S.; Li, R.; Yan, C.; et al. Spatiotemporal characteristics, patterns, and causes of land-use changes in China since the late 1980s. *J. Geogr. Sci.* **2014**, *24* (2), 195−210.
(55) Ma, T.; Zhou, C.; Pei, T.; Haynie, S.; Fan, J. Quantitative estimation of urbanization dynamics using time series of DMSP/OLS

DOI: 10.1021/acs.est.8b05984
Environ. Sci. Technol. 2019, 53, 1822−1833

nighttime light data: a comparative case study from China's cities. *Remote Sens. Environ.* **2012**, *124*, 99−107.
(56) Guan, X.; Wei, H.; Lu, S.; Dai, Q.; Su, H. Assessment on the urbanization strategy in China: Achievements, challenges and reflections. *Habitat Int.* **2018**, *71*, 97−109.
(57) Haas, J.; Ban, Y. Urban growth and environmental impacts in Jing-Jin-Ji, the Yangtze, River Delta and the Pearl River Delta. *ITC J.* **2014**, *30*, 42−55.
(58) Dahiya, B. Cities in Asia, 2012: Demographics, economics, poverty, environment and governance. *Cities* **2012**, *29*, S44−S61.
(59) Wang, T.; Xue, L.; Brimblecombe, P.; Lam, Y. F.; Li, L.; Zhang, L. Ozone pollution in China: a review of concentrations, meteorological influences, chemical precursors, and effects. *Sci. Total Environ.* **2017**, *575*, 1582−1596.
(60) Han, L.; Zhou, W.; Li, W.; Li, L. Impact of urbanization level on urban air quality: a case of fine particles ($PM_{2.5}$) in Chinese cities. *Environ. Pollut.* **2014**, *194*, 163−170.
(61) Chang, Y.; Deng, C.; Dore, A. J.; Zhuang, G. Human excreta as a stable and important source of atmospheric ammonia in the megacity of Shanghai. *PLoS One* **2015**, *10* (12), e0144661.
(62) Rumsey, I.; Cowen, K.; Walker, J.; Kelly, T.; Hanft, E.; Mishoe, K.; Rogers, C.; Proost, R.; Beachley, G.; Lear, G. An assessment of the performance of the Monitor for AeRosols and GAses in ambient air (MARGA): a semi-continuous method for soluble compounds. *Atmos. Chem. Phys.* **2014**, *14* (11), 5639−5658.
(63) Walters, W. W.; Goodwin, S. R.; Michalski, G. Nitrogen stable isotope composition ($\delta^{15}N$) of vehicle-emitted NO_x. *Environ. Sci. Technol.* **2015**, *49* (4), 2278−2285.
(64) Liu, D.; Fang, Y.; Tu, Y.; Pan, Y. Chemical method for nitrogen isotopic analysis of ammonium at natural abundance. *Anal. Chem.* **2014**, *86* (8), 3787−92.
(65) Chang, Y.; Liu, X.; Deng, C.; Dore, A. J.; Zhuang, G. Source apportionment of atmospheric ammonia before, during, and after the 2014 APEC summit in Beijing using stable nitrogen isotope signatures. *Atmos. Chem. Phys.* **2016**, *16* (18), 11635−11647.
(66) Hu, J.; Chen, J.; Ying, Q.; Zhang, H. One-year simulation of ozone and particulate matter in China using WRF/CMAQ modeling system. *Atmos. Chem. Phys.* **2016**, *16* (16), 10333−10350.
(67) Layman, C. A.; Araujo, M. S.; Boucek, R.; Hammerschlag-Peyer, C. M.; Harrison, E.; Jud, Z. R.; Matich, P.; Rosenblatt, A. E.; Vaudo, J. J.; Yeager, L. A.; Post, D. M.; Bearhop, S. Applying stable isotopes to examine food-web structure: an overview of analytical tools. *Biological Reviews* **2012**, *87* (3), 545−562.
(68) Ward, E. J.; Semmens, B. X.; Phillips, D. L.; Moore, J. W.; Bouwes, N. A quantitative approach to combine sources in stable isotope mixing models. *Ecosphere* **2011**, *2* (2), art19.
(69) Zong, Z.; Wang, X.; Tian, C.; Chen, Y.; Fang, Y.; Zhang, F.; Li, C.; Sun, J.; Li, J.; Zhang, G. First Assessment of NO_x sources at a regional background site in North China using isotopic analysis linked with modeling. *Environ. Sci. Technol.* **2017**, *51* (11), 5923−5931.
(70) Parnell, A. C.; Inger, R.; Bearhop, S.; Jackson, A. L. Source partitioning using stable isotopes: coping with too much variation. *PLoS One* **2010**, *5* (3), e9672.
(71) Ward, E. J.; Semmens, B. X.; Schindler, D. E. Including source uncertainty and prior information in the analysis of stable isotope mixing models. *Environ. Sci. Technol.* **2010**, *44* (12), 4645−4650.
(72) Divers, M. T.; Elliott, E. M.; Bain, D. J. Quantification of nitrate sources to an urban stream using dual nitrate isotopes. *Environ. Sci. Technol.* **2014**, *48* (18), 10580−10587.
(73) Blumenthal, S. A.; Chritz, K. L.; Rothman, J. M.; Cerling, T. E. Detecting intraannual dietary variability in wild mountain gorillas by stable isotope analysis of feces. *Proc. Natl. Acad. Sci. U. S. A.* **2012**, *109* (52), 21277−21282.
(74) Rutz, C.; Bluff, L. A.; Reed, N.; Troscianko, J.; Newton, J.; Inger, R.; Kacelnik, A.; Bearhop, S. The ecological significance of tool use in new Caledonian crows. *Science* **2010**, *329* (5998), 1523−1526.
(75) Palacio, S.; Azorín, J.; Montserrat-Martí, G.; Ferrio, J. P. The crystallization water of gypsum rocks is a relevant water source for plants. *Nat. Commun.* **2014**, *5*, 4660.
(76) Felix, J. D.; Elliott, E. M.; Gish, T. J.; McConnell, L. L.; Shaw, S. L. Characterizing the isotopic composition of atmospheric ammonia emission sources using passive samplers and a combined oxidation-bacterial denitrifier approach. *Rapid Commun. Mass Spectrom.* **2013**, *27* (20), 2239−2246.
(77) Chang, Y.; Ma, H. Comment on "Fossil fuel combustion-related emissions dominate atmospheric ammonia sources during severe haze episodes: Evidence from ^{15}N-stable isotope in size-resolved aerosol ammonium". *Environ. Sci. Technol.* **2016**, *50* (19), 10765−10766.
(78) Carslaw, D. C.; Beevers, S. D.; Ropkins, K.; Bell, M. C. Detecting and quantifying aircraft and other on-airport contributions to ambient nitrogen oxides in the vicinity of a large international airport. *Atmos. Environ.* **2006**, *40* (28), 5424−5434.
(79) Carslaw, D. C.; Ropkins, K. Openair — An R package for air quality data analysis. *Environ. Modell. Softw.* **2012**, *27*, 52−61.
(80) Chang, Y.; Deng, C.; Cao, F.; Cao, C.; Zou, Z.; Liu, S.; Lee, X.; Li, J.; Zhang, G.; Zhang, Y. Assessment of carbonaceous aerosols in Shanghai, China − Part 1: long-term evolution, seasonal variations, and meteorological effects. *Atmos. Chem. Phys.* **2017**, *17*, 9945−9964.
(81) Chang, Y.; Huang, K.; Xie, M.; Deng, C.; Zou, Z.; Liu, S.; Zhang, Y. First long-term and near real-time measurement of trace elements in China's urban atmosphere: temporal variability, source apportionment and precipitation effect. *Atmos. Chem. Phys.* **2018**, *18*, 11793−11812.
(82) Meng, Z. Y.; Lin, W. L.; Jiang, X. M.; Yan, P.; Wang, Y.; Zhang, Y. M.; Jia, X. F.; Yu, X. L. Characteristics of atmospheric ammonia over Beijing, China. *Atmos. Chem. Phys.* **2011**, *11* (12), 6139−6151.
(83) Cao, J. J.; Zhang, T.; Chow, J. C.; Watson, J. G.; Wu, F.; Li, H. Characterization of Atmospheric Ammonia over Xi'an, China. *Aerosol Air Qual. Res.* **2009**, *9* (2), 277−289.
(84) Ju, X. T.; Xing, G. X.; Chen, X. P.; Zhang, S. L.; Zhang, L. J.; Liu, X. J.; Cui, Z. L.; Yin, B.; Christie, P.; Zhu, Z. L.; Zhang, F. S. Reducing environmental risk by improving N management in intensive Chinese agricultural systems. *Proc. Natl. Acad. Sci. U. S. A.* **2009**, *106* (9), 3041−3046.
(85) Shangguan, W.; Dai, Y.; Liu, B.; Zhu, A.; Duan, Q.; Wu, L.; Ji, D.; Ye, A.; Yuan, H.; Zhang, Q.; Chen, D.; Chen, M.; Chu, J.; Dou, Y.; Guo, J.; Li, H.; Li, J.; Liang, L.; Liang, X.; Liu, H.; Liu, S.; Miao, C.; Zhang, Y. A China data set of soil properties for land surface modeling. *J. Adv. Model. Earth Syst.* **2013**, *5* (2), 212−224.
(86) Zhao, X.; Xie, Y. X.; Xiong, Z. Q.; Yan, X. Y.; Xing, G. X.; Zhu, Z. L. Nitrogen fate and environmental consequence in paddy soil under rice-wheat rotation in the Taihu lake region, China. *Plant Soil* **2009**, *319* (1), 225−234.
(87) Kang, C. M.; Lee, H. S.; Kang, B. W.; Lee, S. K.; Sunwoo, Y. Chemical characteristics of acidic gas pollutants and $PM_{2.5}$ species during hazy episodes in Seoul, South Korea. *Atmos. Environ.* **2004**, *38* (28), 4749−4760.
(88) Gong, L.; Lewicki, R.; Griffin, R. J.; Flynn, J. H.; Lefer, B. L.; Tittel, F. K. Atmospheric ammonia measurements in Houston, TX using an external-cavity quantum cascade laser-based sensor. *Atmos. Chem. Phys.* **2011**, *11* (18), 9721−9733.
(89) Singh, S.; Kulshrestha, U. C. Abundance and distribution of gaseous ammonia and particulate ammonium at Delhi, India. *Biogeosciences* **2012**, *9* (12), 5023−5029.
(90) Singh, S.; Kulshrestha, U. C. Rural versus urban gaseous inorganic reactive nitrogen in the Indo-Gangetic plains (IGP) of India. *Environ. Res. Lett.* **2014**, *9* (12), 125004.
(91) Van Damme, M.; Clarisse, L.; Heald, C. L.; Hurtmans, D.; Ngadi, Y.; Clerbaux, C.; Dolman, A. J.; Erisman, J. W.; Coheur, P. F. , Global distributions, time series and error characterization of atmospheric ammonia (NH_3) from IASI satellite observations. *Atmos. Chem. Phys.* **2014**, *14* (6), 2905−2922.
(92) Clarisse, L.; Clerbaux, C.; Dentener, F.; Hurtmans, D.; Coheur, P. F. Global ammonia distribution derived from infrared satellite observations. *Nat. Geosci.* **2009**, *2* (7), 479−483.
(93) Wang, S.; Nan, J.; Shi, C.; Fu, Q.; Gao, S.; Wang, D.; Cui, H.; Saiz-Lopez, A.; Zhou, B. Atmospheric ammonia and its impacts on

DOI: 10.1021/acs.est.8b05984
Environ. Sci. Technol. 2019, 53, 1822−1833

regional air quality over the megacity of Shanghai, China. *Sci. Rep.* **2015**, *5* (1), 15842.
(94) Dewes, T. Effect of pH, temperature, amount of litter and storage density on ammonia emissions from stable manure. *J. Agric. Sci.* **1996**, *127* (4), 501−509.
(95) Tanner, P. A. Vehicle-related ammonia emissions in Hong Kong. *Environ. Chem. Lett.* **2009**, *7* (1), 37−40.
(96) Perrino, C.; Catrambone, M.; Di Bucchianico, A. D. M.; Allegrini, I. Gaseous ammonia in the urban area of Rome, Italy and its relationship with traffic emissions. *Atmos. Environ.* **2002**, *36* (34), 5385−5394.
(97) Hu, Q.; Zhang, L.; Evans, G. J.; Yao, X. Variability of atmospheric ammonia related to potential emission sources in downtown Toronto, Canada. *Atmos. Environ.* **2014**, *99*, 365−373.
(98) Sommer, S. G.; Olesen, J. E.; Christensen, B. T. Effects of temperature, wind speed and air humidity on ammonia volatilization from surface applied cattle slurry. *J. Agric. Sci.* **1991**, *117* (1), 91−100.
(99) Cheng, H.; Hu, Y.; Reinhard, M. Environmental and Health Impacts of Artificial Turf: A Review. *Environ. Sci. Technol.* **2014**, *48* (4), 2114−2129.
(100) Asman, W. A.; Sutton, M. A.; Schjørring, J. K. Ammonia: Emission, atmospheric transport and deposition. *New Phytol.* **1998**, *139* (1), 27−48.
(101) Behera, S. N.; Sharma, M.; Aneja, V. P.; Balasubramanian, R. Ammonia in the atmosphere: a review on emission sources, atmospheric chemistry and deposition on terrestrial bodies. *Environ. Sci. Pollut. Res.* **2013**, *20* (11), 8092−8131.
(102) Phillips, D. L.; Gregg, J. W. Source partitioning using stable isotopes: coping with too many sources. *Oecologia* **2003**, *136* (2), 261−269.
(103) Chang, Y.; Zhang, Y.; Tian, C.; Zhang, S.; Ma, X.; Cao, F.; Liu, X.; Zhang, W.; Kuhn, T.; Lehmann, M. F. Nitrogen isotope fractionation during gas-to-particle conversion of NO_x to NO_3^- in the atmosphere − implications for isotope-based NO_x source apportionment. *Atmos. Chem. Phys.* **2018**, *18* (16), 11647−11661.

DOI: 10.1021/acs.est.8b05984
Environ. Sci. Technol. 2019, 53, 1822−1833